

Effects of bottom aerator and self aeration in steep chute spillways on cell center finite volume solution of depth-averaged flow

S.R. Sabbagh-Yazdi, H. Rezaei-Manizani and N.E. Mastorakis

Abstract—In this paper the effects of air concentrations on the numerical computation of spill flow parameters in chute canals are investigated. The flow parameters in terms of depth averaged velocity components parallel to the bottom surface and flow depth are computed by solution of depth average continuity and momentum equations using cell centre finite volume method. The effect of self aeration from the water surface on the flow parameters are assessed by comparison of computed results with the observations on the AVIMORE chute spillway. The best experimental relations for simulating the entrainment of air into the flow on chute spillways have been chosen. Then, the model is completed for aeration from a bottom aerator and results of air concentration distribution are compared with the reported measurements on a physical model. In order to provide better understanding of the velocity and air concentration, the vertical distribution profiles of these parameters are plotted from the multi layer treatments of depth averaged computed results.

Keywords— Finite Volume Solution, Depth-Averaged Equations, Steep Slope Chutes, Self Aeration and Bottom Aerator,

I. INTRODUCTION

Spillways, chutes, and bottom outlets are important hydraulic structures for dam safety. Due to high velocities combined with low pressures, cavitation may occur on the chute bottom and side walls and cause major damage, or even endanger the dam stability. Major damage was observed, for example, on the Karun dam in Iran in 1977 and the Glen Canyon dam in Colorado in 1983.

Peterka [1] provided evidence that an average air concentration \bar{C} of some 5% reduces the cavitations risk almost completely. The elastic properties of water change dramatically with the presence of air bubbles. Even if the

amount of air needed for cavitations protection was questioned throughout the past 50 years, scientists agreed that a small amount of air close to the chute bottom reduces the risk of cavitations damage significantly (Kramer 2004) [1].

Therefore, the process of aeration in spillways and steep chutes has historically been of interest to hydraulic engineers because of the “bulking” effect the entrained air has on the depth of flow. The amount of “bulking” is a necessary design parameter in determining the height of spillway or chute sidewalls. Engineers have also been interested in eliminating or minimizing cavitations damage caused by high velocity flow in spillways, chutes, and channels [1].

Self-aeration is a phenomenon which can be observed in high velocity flows on spillways or in steep channels. The flow turns frothy and white with entrained air when aeration is initiated. Studies of self-aerated spillway flow have shown that the turbulent boundary layer, caused by the spillway surface, initiates air entrainment when it intersects the water surface at the “point of inception”. For some distance, the flow is developing, i.e., there is a net flux of air into the water. When the air bubbles are transported to their maximum depth in the water, the flow is considered fully aerated, but continues to entrain more air and thus is still developing. At some long distance along the spillway, uniform conditions are approached. Thereafter, there is no significant change in the hydraulic or air transport characteristics [2].

Bottom aerators may be considered for the cases that the air entrainment from the water surface does not satisfy the minimum air concentration requirements, particularly near the chute bottom. The principle aerator types consist of deflectors, grooves, offsets, and combinations of these. Usually a combination of the three basic shapes provides the best design. The ramp dominates the operation at small discharges, the groove provides space for air supply, and the offset enlarges the jet trajectory for higher discharges [1, 2].

Recently the first author of the paper succeeded to develop a depth average finite volume solver which solves spilling flow from the dam reservoir to the steep chute spillways with variable bed slope. This model computes velocity profiles along the water depth by application of empirical relations on the layers parallel to the bed surface [3]. The compression of the results of this two dimensional flow solver with the results of a commercial three dimensional flow solver showed that,

Manuscript received January 3, 2008; Revised version received May 1, 2008

Saeed-Reza Sabbagh-Yazdi Civil Engineering Department, KN Toosi University of Technology, No.1346 Valiasr Street, 19697- Tehran, IRAN(e-mail: SYazdi@kntu.ac.ir).

Habib Rezaei-Manizani, Civil Engineering Department, KN Toosi University of Technology, No.1346 Valiasr Street, 19697- Tehran, IRAN(e-mail: Rmanizani@gmail.com).

Nikos E. Mastorakis, is Professor of Military Institutes of University Education (ASEI) Hellenic Naval Academy, Terma Chatzikyriakou 18539, Piraeus, GREECE

the results of the developed two dimensional solver is acceptable for the super-critical flows in chute spillways without vertical curvature [4]. Then, the model developed for computation of self-aeration from water surface and considering the air concentration distribution on the computed flow variables [5].

The objective of this paper is modeling the effect of the bottom aeration in the chute spillway considering the self aeration effects. Computations of supercritical flow on steep slope chute canals are performed considering the effects of mean air concentration from self aeration from the water surface and aerator in the chute bottom. Hence, the reduction in global stresses and increasing of the flow depth bulking due to the free surface aeration and bottom aerator are simultaneously considered with solving the flow equations at each computational step. The computed results have been compared with self-aeration observation on the AVIMORE chute spillway (Cain 1987) and reported measurements for a physical model with bottom aerator (Kramer 2004).

II. FLOW REGIMES ON CHUTES

When water particles move perpendicular to the main flow direction, they must have an adequate kinetic energy to overcome the restraining surface tension to be ejected out of the flow. Volkart (1980) described the general method with droplets being projected above the water surface and than falling back, thereby entraining air bubbles into the flow. A flow is considered fully turbulent if boundary layer thickness along the chute is equal to the flow depth. In high velocity flows on spillways, the turbulent boundary layer reaches the flow surface at the “point of inception”, initiating air entrainment into the flow stream. Observations have shown that there is a developing flow region after the inception point of air entrainment. For some distance in the developing region, there is a region of partially aerated flow, until the air bubbles penetrate to their maximum depth in the water and the flow becomes fully aerated. After the developing region, there is a fully developed aerated flow region where uniform conditions have been obtained [1].

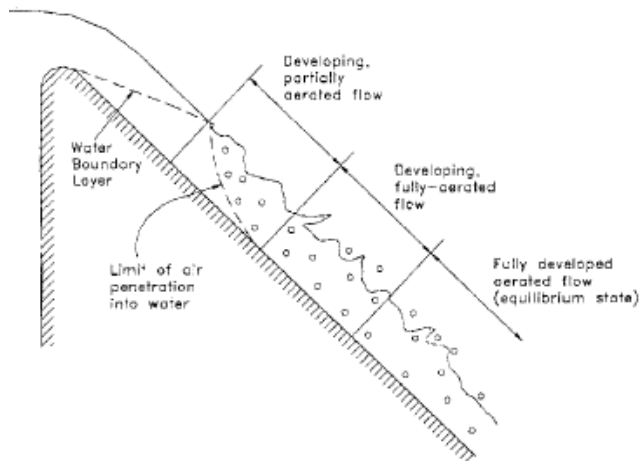


Fig.1 Region of developing flow

The typical behavior of the average air concentration is shown Figure 2, it was classified in: (1) Inflow air concentration \bar{C}_0 , (2) Air detrainment region $\bar{C}_{90,det}$ between \bar{C}_0 , and (3) Minimum air concentration $\bar{C}_{90,min}$, (4) Air entrainment region $\bar{C}_{90,ent}$ between $\bar{C}_{90,min}$, and (5) Uniform air concentration $\bar{C}_{90,u}$. Figure 6.1 shows an aerator and the downstream flow region. The air is entrained from: (1) The bottom cavity due to the jet deflection, (2) The free surface in the centre region by turbulence effects [1, 2].

The region between the lower jet nappe and the chute bottom directly downstream of the aerator is called the air cavity, with an air concentration $C = 100\%$. The free surface air entrainment direct at the aerator must be considered with special attention. The pressure field changes from a reasonable hydrostatic profile p_{hyd} upstream of the aerator to negative pressure $p < 0$ in the cavity immediately downstream of the deflector before it impinges with a high bottom pressure $p > p_{hyd}$ at the point of inception. This highly non-hydrostatic pressure field causes turbulence which leads to an air entrainment from both, the cavity and the free surface, direct at the aerator. This behavior is qualitatively shown in Figure 3. The air entrainment in this region is highly developing and therefore not considered for the present data analysis [1].

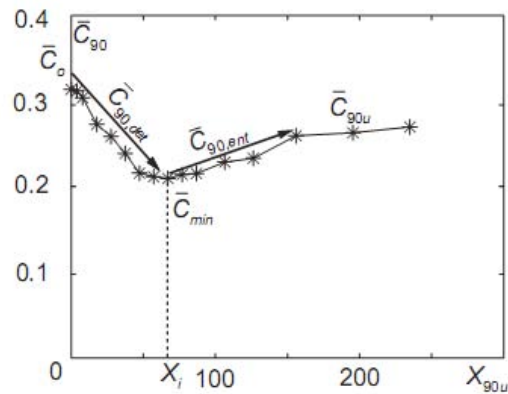


Fig.2 Typical average air concentration development C_{90} as a function of non-dimensional distance $X_{90,u}$ [1]

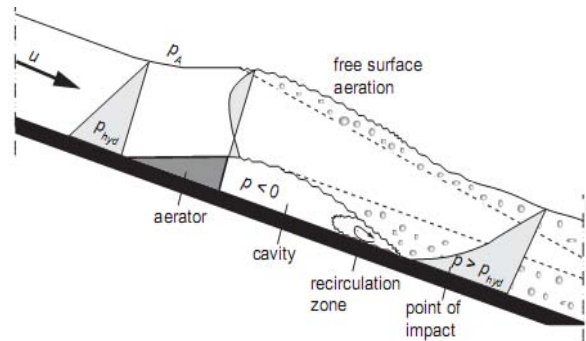


Fig.3 Region of developing flow (Kramer, 2004) [1]

III. MATHEMATICAL MODEL

A. Flow Equations

The water phase mathematical equations are shallow water equations modified for a coordinate system with an axis normal and two axes(x' and y) parallel to the bed surface.

$$\frac{\partial h'}{\partial t} + \frac{\partial(h'u')}{\partial x'} + \frac{\partial(h'v)}{\partial y} = 0 \tag{1-a}$$

$$\begin{aligned} &\frac{\partial(h'u')}{\partial t} + \frac{\partial(u'h'u')}{\partial x'} + \frac{\partial(vh'u')}{\partial y} + \frac{\partial}{\partial x'} \left[h' \frac{gh' \cos \alpha}{2} \right] \\ &= gh' \sin \alpha - gh' S_{fx'} \end{aligned} \tag{1-b}$$

$$\begin{aligned} &\frac{\partial(h'v)}{\partial t} + \frac{\partial(u'h'v)}{\partial x'} + \frac{\partial(vh'v)}{\partial y} + \frac{\partial}{\partial y} \left[h' \frac{gh' \cos \alpha}{2} \right] \\ &= -gh' S_{fy} \end{aligned} \tag{1-c}$$

In which:

$$\begin{aligned} S_{fx'} &= \frac{n^2 u' \sqrt{u'^2 + v^2}}{h'^{4/3}} \\ S_{fy} &= \frac{n^2 v \sqrt{u'^2 + v^2}}{h'^{4/3}} \end{aligned} \tag{2}$$

In these equations x' is the axis tangential to the chute slope and y is the same as the y axis in the global coordinate system; u' and v are the velocity components in x' and y directions, respectively; h' is the flow depth perpendicular to the chute bed surface and g is gravity acceleration; α is the chute angle; S_{fx'} and S_{fy} are the bed surface friction slopes in x' and y directions, respectively and n is Manning's friction coefficient [3].

B. Self Aeration Relations

Wilhelm's et al. (2005) gave a relationship for defining mean air concentration [6]:

$$\bar{C}_e = \bar{C}_\infty (1 - e^{-0.010 X^* / Y_i}) \tag{3}$$

Where \bar{C}_e is the mean air concentration, X^* is the distance from inception point along the chute slope, Y_i is the flow depth at the point of inception, and \bar{C}_∞ as follows:

$$\begin{aligned} \bar{C}_\infty &= 0.626(1 - e^{-0.0356(\theta - 10.9)}) + 0.23 \\ &; 11 \leq \theta \leq 75 \end{aligned} \tag{4}$$

Where θ is the chute angle.

Air concentration profiles C(y), by Chanson (1995) expressed by [7]:

$$C = 1 - \tanh^2 \left(K' - \frac{y'}{2D'} \right) \tag{5}$$

Where; $y' = \frac{Y}{Y_{90}}$

To define K' and D', the following relationships have been fit to experimental data:

$$D' = 3.5722C_e^3 - 2.3456C_e^2 + 1.15799C_e - 0.0166 \tag{6}$$

(R² = 0.999)

$$K' = 0.7766C_e^{-0.9877} \tag{7}$$

(R² = 0.9978)

The relations used for defining the inception point distance from the crest along the chute are as follows.

Wood et al (1983) derived [8]:

$$\frac{L_{b1}}{K_s} = 13.6 (\sin \alpha)^{0.0796} (F_*)^{0.713} \tag{8}$$

Where; $F_* = \frac{q_w}{\sqrt{gK_s^3 \sin \alpha}}$

Fernando et al (2002) derived:

$$L_{b1} = \left(\frac{q}{0.05642k_s^{0.056} (\sin \alpha)^{0.34}} \right)^F \tag{9}$$

Where; $F = (1.46443k_s^{0.0054} (\sin \alpha)^{0.0027})^{-1}$

Where L_{b1} is the inception point distance from the crest along the chute are as follows, K_s is equivalent sand roughness, q_w is specific water discharge and α is the chute angle.

The relations used for defining the mixture flow depth at the point of inception are as follows.

Wood et al (1983) derived [8]:

$$\frac{d_{b1}}{K_s} = \frac{0.223}{(\sin \alpha)^{0.04}} (F_*)^{0.643} \quad (10)$$

Where d_{b1} is depth at the point of inception and $F_* = \frac{q_w}{\sqrt{gK_s^3 \sin \alpha}}$.

C. Bottom Aerator Relations

Kramer (2004) gave a relationship for defining mean air concentration for aerator flow [1, 9]:

1) Air detrainment region $\bar{C}_{90,det}$:

$$\bar{C}_{90,det} = 0.0085(\sin \alpha - 1)X_{90u} + \bar{C}_0 \quad (11)$$

2) Minimum air concentration $\bar{C}_{90,min}$:

$$\bar{C}_{90,min} = 0.015 \left(\frac{F_0 + F_{\bar{C}_{min}}}{2} \right) \quad (12)$$

3) Air entrainment region $\bar{C}_{90,ent}$:

$$\bar{C}_{90,ent} = \bar{C}_{90u} \tanh(0.004X_{90u}) \quad (13)$$

4) Uniform air concentration $\bar{C}_{90,u}$:

$$\bar{C}_{90u} = \frac{1}{3} (\sin \alpha)^{0.25} \quad (14)$$

Where F_0 is inflow Froude number $F_{\bar{C}_{min}}$ is the Froude number at the inception point, $X_{90u} = x/h_{90}$ where x is distance of aerator and h_{90} is uniform mixture flow depth and α is the chute angle.

The reduction coefficient is defined by the following relation proposed by Wood et al (1991):

$$f = -2.144C^2 + 0.335C + 0.99 \quad (15)$$

IV. NUMERICAL SOLUTION & FLOW EQUATION

In the numerical model, the shallow water equations have been modified for a coordinate system with an axis normal and two axes(x' and y) parallel to the bed surface. The depth and velocity values are depth-averaged values computed on a triangular unstructured mesh using the finite volume method.

The equations have been converted to discrete form using cell centre method. The experimental relations have been added to the model to compute the inception point distance from the crest, the flow depth in this section and the depth-averaged air concentration in each joint. Then the velocity and air concentration distributions in flow depth have been obtained using experimental relations. Can write the formed vector in before stage the shallow water equations:

$$\frac{\partial Q}{\partial t} + \frac{\partial E}{\partial x} + \frac{\partial F}{\partial y} = S \quad (16)$$

A. Finite Volume Formulation

Application of the Green' theorem in equation (17) and the integrated equation form is:

$$\int_{\Omega} \left(\frac{\partial Q}{\partial t} + \frac{\partial E}{\partial x} + \frac{\partial F}{\partial y} \right) dx dy = \int_{\Omega} S dx dy \quad (18)$$

$$Q^{n+1} = Q^n - \frac{\Delta t}{\Omega} \sum_{k=1}^N (\bar{E} \Delta x - \bar{F} \Delta y)_k + S \Delta t \quad (19)$$

Where Ω is the area of the control volume, Q^{n+1} is the value of Q^n to be computed after Δt and N in the cell centre method solves the governing equations for the centre of each triangular cell as a control volume. Therefore in equation (19) N is the number of boundary sides of the triangular cell and the flow parameters are solved at centre of the cell. Therefore, the computed parameters should be transferred to the nodal points of the cell sides [4].

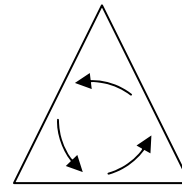


Fig.4 control volume cell centre

B. Boundary Conditions

Free slip impermeable condition is considered along side wall boundaries by enforcing zero normal velocity components (at nodal points of the wall edges).

The flow type in the outflow boundary is free from imposing flow parameters and upstream velocity and depth is imposed at inflow boundary. Therefore, inflow boundary conditions are imposed manually, by imposing following flow parameters:

For Aviemor test: $u_0 = 11.07 \frac{m^2}{s}$, $h_0 = 0.2m$

For physical model test:

$$Fr=8: q = 0.5 \frac{m^3}{s} \rightarrow F_0 = \frac{q}{\sqrt{gh_0^3}} = 8 \Rightarrow h_0 = 0.074m$$

$$\rightarrow u_0 = \frac{q}{h_0} \Rightarrow u_0 = 6.796 \frac{m}{s}$$

In present work, in order to compute the average air concentration distribution using the depth average water flow parameters, modeling strategy is used: Simultaneous computation of the free surface aeration flow and bottom aerator parameters (air concentration) and solving the flow equation. In this strategy the effect of aeration (i.e. reduction in global stresses and depth bulking) on flow parameters are considered at each computational step of numerical solution.

V. SELF AERATION RESULTS

Air concentration and velocity compared with data observation in stations 503 of Aviemore spillway, with distances of 15 m from the crest of the spillway (Fig.5).

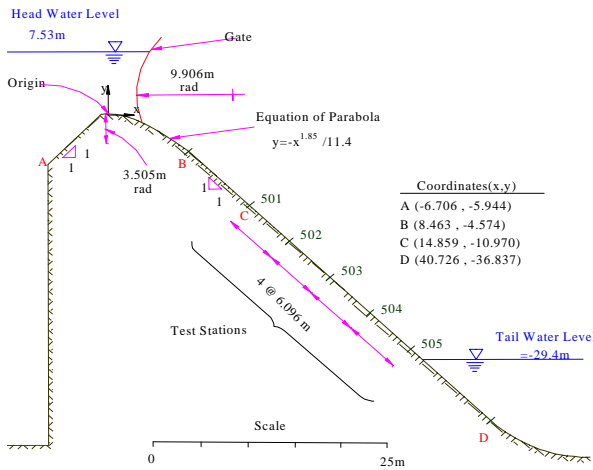


Fig.5 Aviemore spillway and measuring stations

A. Flow Solver Results

Figure 6 shows the triangular unstructured mesh utilized for finite volume solution of flow parameter of Aviemore spillway chute. This mesh includes 377 nodes, 642 triangular and 1018 edges.

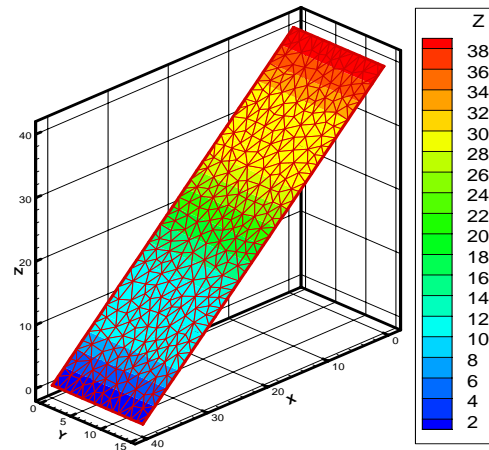


Fig.6: Mesh for Aviemore spillway chute

Figures 7 and 8 show color coded maps of depth and depth averaged velocity vectors on aerated flow in the Aviemore chute spillway.

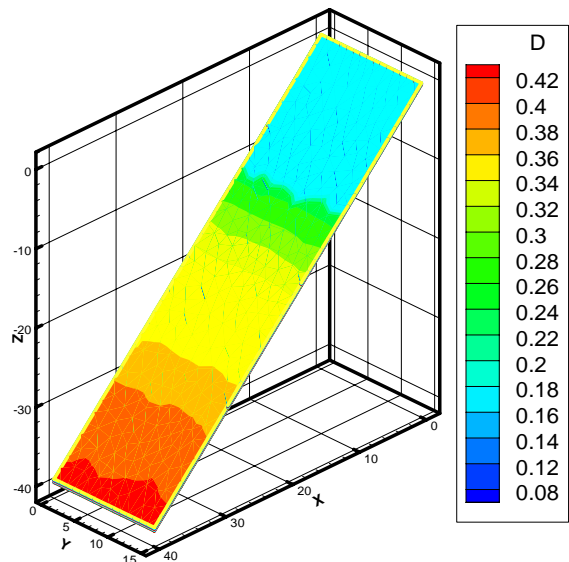


Fig.7: Depth color coded map for Aviemore spillway chute

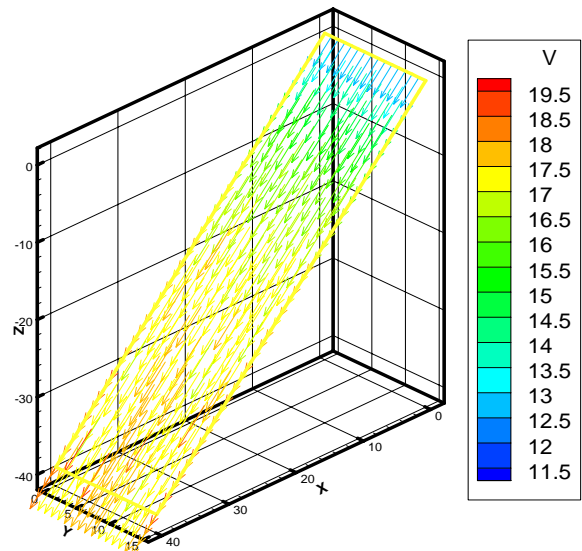


Fig.8 Velocity color coded map for Aviemore spillway chute flow

0.445%	0.25%
--------	-------

B. Inception Point of Aeration

The errors on the computing the location of the inception point and the flow depth in that section are tabulated in the following tables.

Table.1 Errors on computed inception point distance from the starting point of super critical flow

Fernando et al (2002)		Wood et al (1983)	
Value(m)	Errors	Value(m)	Errors
14.78	5.57%	11.37	18.79%

Table.2 Errors of computed depth at inception point

Bauer (1954)		Wood et al (1983)	
Value(m)	Errors	Value(m)	Errors
0.136	10.53%	0.142	6.58%

By comparison between the mean air concentration computed by modeling, it can be concluded that the best relation for inception point distance and depth are those proposed by Fernando's and Wood's, respectively.

C. Mean Air Concentration

Figure 9 shows the field measurement of the air concentration profile in flow depth in station 503 [7]. The mean air concentration is computed by integrating on the air concentration profile at that station.

$$c_{mean} = \frac{1}{h} \int_0^h cdh$$

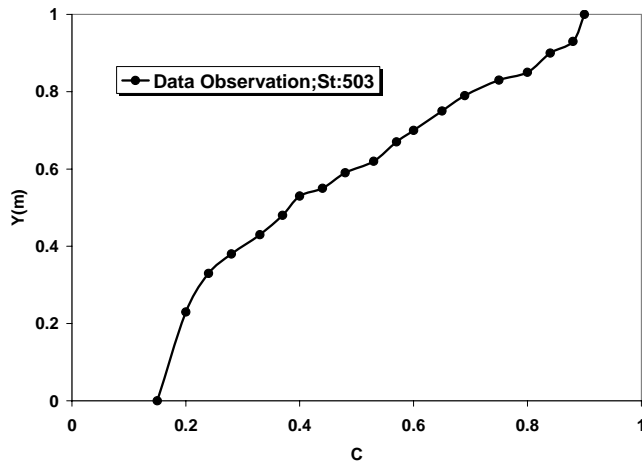


Fig.9 Air concentration - flow depth in station 503 [7]

Table.3 Errors on computed mean air concentration

Value	Errors
-------	--------

D. Mean Aerated Flow Velocity

Figure 10 shows the field measurement of the velocity profile in flow depth in station 503 [7]. Here the mean velocity is computed by integrating on the velocity profile at that station.

$$V_{mean} = \frac{1}{h} \int_0^h vdh$$

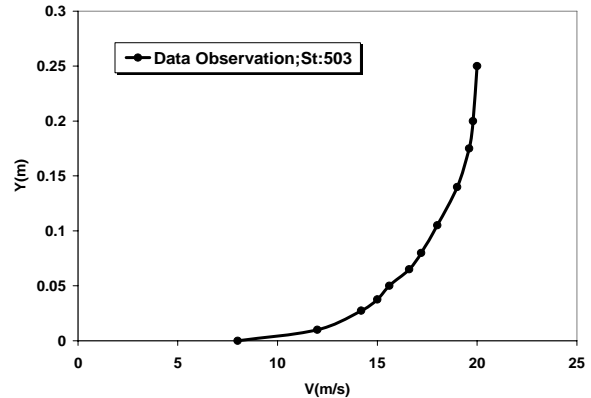


Fig. 10 Velocity - flow depth in station 503 [5]

Table.4 Errors on computed average velocities

Value(m/s)	Errors
17.79	0.8%

VI. BOTTOM AERATION RESULTS

Bottom aeration compared with the reported measurements on a physical model [9] in point of minimum air concentration $\bar{C}_{90,min}$ (Fig.11).

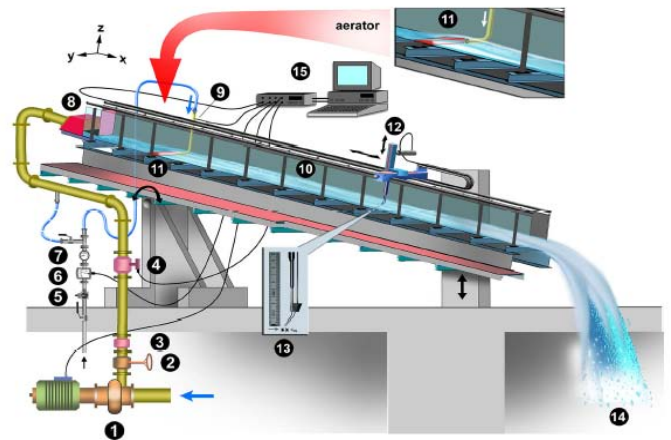


Fig.11 Physical model including the measuring system for bottom aerator [9]

A. Flow Solver Results

Figure 12 shows the triangular unstructured mesh utilized for finite volume solution of flow parameter of physical modeling spillway chute. This mesh includes 478 nodes, 742

triangular and 1125 edges.

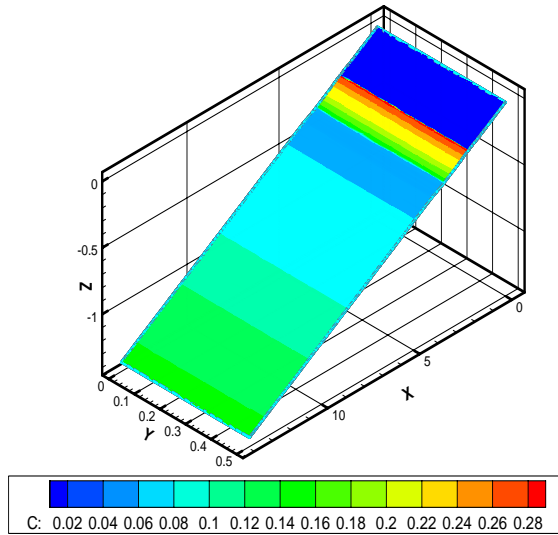


Fig.12 Depth color coded map for aerator flow

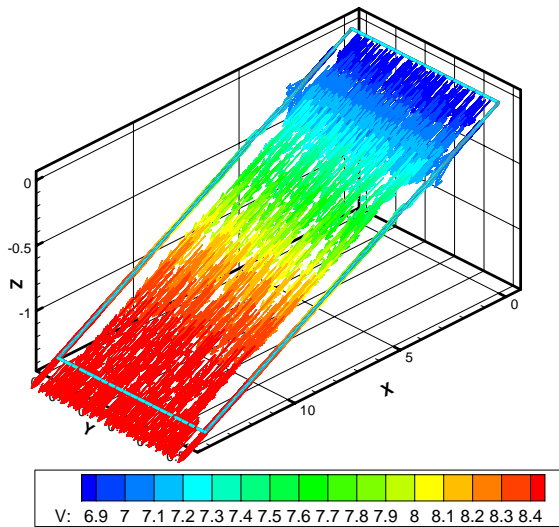


Fig.13 Velocity color coded map for aerator

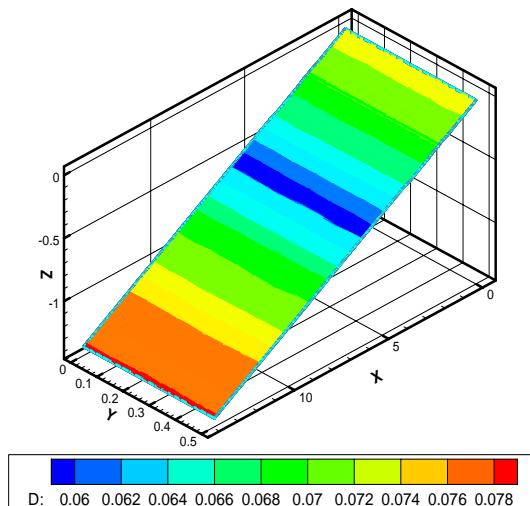


Fig.14 Air concentration color coded map for aerator flow

B. Air Concentration Profiles Computation for aerator flow

Comparison of the error values computed by three modeling strategies shows that consideration of the water-air density variations in the momentum equations produces negligible differences in computed values. Here, the program is run for Fernando's relation for inception point location, Wood's relation for flow depth at the point of inception, Wilhelm's relation for mean air concentration of surface flow and Kramer's relation for average air concentration for aerator flow.

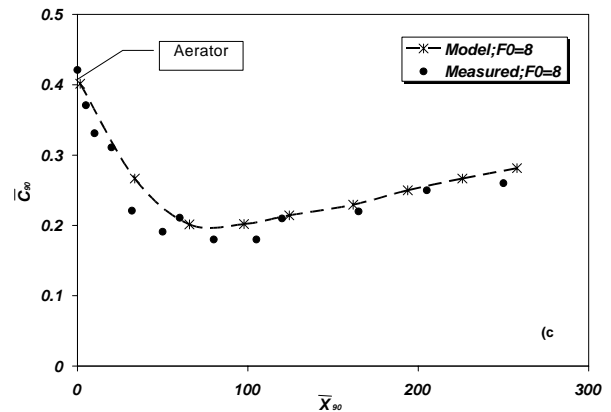
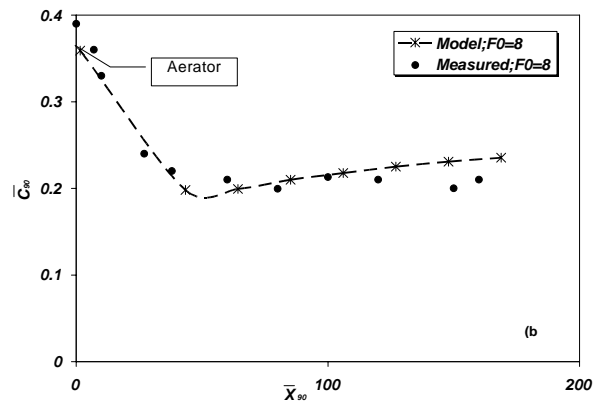
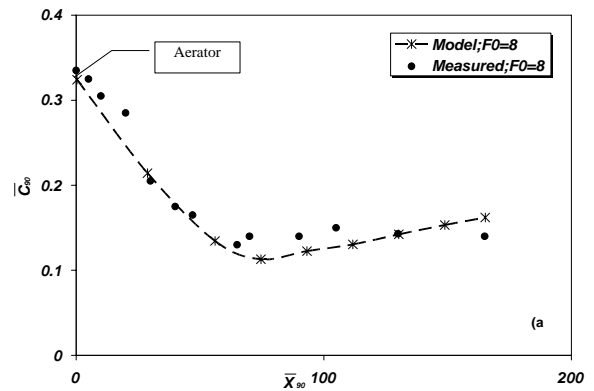


Fig.15 Average air concentration development \bar{C}_{90} as a function of non-dimensional distance X_{90} for aerator flow for various slopes a) $S_0=10\%$, b) $S_0=30\%$ and c) $S_0=50\%$

Table.5 Errors on computed Minimum air concentration

Slope	Minimum air concentration	Minimum air concentration	Errors
10 %	0.140%	0.144%	2.78 %
30 %	0.2%	0.21%	5.0%
50 %	0.21%	0.20%	2.0%

VII. CONCLUSION

The numerical solution of flow on steep chute spillway has been carried out using shallow water equations modified in inclined coordinate system. Experimental relations for air entrainment from water surface and bottom aerator have been used for computing distribution of mean air concentration using the results of the numerical flow solver.

Computations of supercritical flow on steep slope chute canals are performed considering the effects of mean air concentration from self aeration from the water surface and aerator in the chute bottom. In the present modeling method, the reduction in global stresses and increasing of the flow depth bulking due to the free surface aeration and bottom aerator are simultaneously considered with solving the flow equations at each computational step.

In order to verify the results of the developed model, self aeration effects on numerical solution is verified by comparison of the computed flow parameters with the reported observations in the AVIMORE chute spillway, and the effects of bottom aerator on computed flow field are assessed by comparison of the results of numerical flow solver with the measurements on a physical model.

The comparison of the results of the model (which considers the effects of aeration from the water surface and bottom aerator in a simultaneous manner) with the field and laboratory measurements ends up with following conclusions:

- Relation 9 for defining inception point location (proposed by Fernando 2002) matches nicely with the developed flow solver.
- Relation 10 for defining flow depth at the inception point (proposed by Wood 1983) produces good results in conjunction with the depth averaged flow solver.
- Relation's Kramer for bottom aerator produces good results in conjunction with the utilized flow solver.
- Simultaneous computing the mean air concentration and solving the flow equations at each computational step results in more accurate computation of average velocity.
- Solving depth average flow equations (even with simple turbulent models like zero equation model) can produce realistic results when the effects of air concentration on global stresses reduction and flow depth bulking are considered.

- Comparison of the computed velocities shows that the effect of water-air density variations on formation of computed flow parameters is negligible.

REFERENCES

- [1] K. Kramer, "Development of Aerated Chute Flow" Doctoral Thesis ETH No. 15428; Dipl.-Ing. Technical University of Darmstadt (TUD), 2004.
- [2] H. Chanson, "Uniform Aerated Chute Flow – Discussion," Journal of Hydraulic Engineering, ASCE, Vol. 118, No. 6, 1992, pp. 944-945 (ISSN 0733-9429).
- [3] SR. Sabbagh-Yazdi, M. Zounemat-Kermani and N.E. Mastorakis, "Velocity Profile over Spillway by Finite Volume Solution of Sloping Depth Averaged Flow" WSEAS Journal of Applied and Theoretical Mechanics, Issue 3, Vol.2, 2007, pp.85-94.
- [4] SR. Sabbagh-Yazdi, H. Rezaei-Manizani and N.E. Mastorakis, "Multi-Layer Computation of Coupled Finite Volume Solution of Depth-Averaged Flow in Steep Chute Spillways Considering Air Concentration Effects," Journal of Fluid Mechanics, Issue 4, Volume 2, 2007, pp 244-249
- [5] SR. Sabbagh-Yazdi, F. Rostami, H. Rezaei-Manizani and N.E. Mastorakis, "Comparison of the Results of 2D and 3D Numerical Modeling of Flow over Spillway Chutes with Vertical Curvatures" International Journal of computers, Issue 4, Volume 1, 2007, pp 296-302.
- [6] S. Wilhelm, "Bubbles and Waves Description of Self-Aerated Spillway Flow" Journal of Hydraulic Research Vol. 43, No. 5, 2005, pp.522-53.
- [7] H. Chanson, "Air Concentration Distribution in Self-Aerated Flow Discussion" Journal of Hydraulic Engineering, Res., IAHR, Vol. 33, No. 4, 1995, pp. 586-588.
- [8] IR. Wood, and P. Cain, "Measurements of Self-Aerated Flow on Spillways" Journal of Hydraulic Div., 107, HY11, 1983, pp. 1425-1444.
- [9] K. Kramer, W. Hager, and H. Minor, "Development of Air Concentration on Chute Spillways" Journal of Hydraulic Engineering, ASCE, 2006, pp.908-915.

First Author's biography may be found in following site:

<http://sahand.kntu.ac.ir/~syazdi/> 3rd Author's: wseas.org/mastorakis